

Highly Stable Si–C Linked Functionalized Monolayers on the Silicon (100) Surface

A. B. Sieval,[†] A. L. Demirel,^{‡,§} J. W. M. Nissink,^{||} M. R. Linford,[⊥]
J. H. van der Maas,^{||} W. H. de Jeu,[‡] H. Zuilhof,[†] and E. J. R. Sudhölter^{*,†}

Laboratory of Organic Chemistry, Department of Biomolecular Sciences, Wageningen Agricultural University, Dreijenplein 8, 6703 HB Wageningen, The Netherlands, FOM–Institute for Atomic and Molecular Physics, Kruislaan 407, 1098 SJ Amsterdam, The Netherlands, Department of Analytical Molecular Spectrometry, Faculty of Chemistry, Utrecht University, Sorbonnelaan 16, 3584 CA Utrecht, The Netherlands, and Rohm and Haas Company, Bristol, Pennsylvania 19007

Received October 20, 1997. In Final Form: December 18, 1997

Monolayers that are bonded via a covalent Si–C bond are prepared on a silicon(100) surface by reaction of a 1-alkene with the hydrogen-terminated silicon surface. The monolayers have been analyzed by infrared spectroscopy, X-ray reflectivity, and water contact angle measurements and display a remarkably high thermal stability. The reaction also works well for ω -functionalized 1-alkenes, provided that the functional group is properly protected. After formation of the monolayer, the protecting group can be easily removed without noticeable disturbance of the monolayer integrity, and the now reactive sites at the monolayer can be used for further functionalization, as has been shown in the case of ester-protected alcohol and carboxylic acids. Functional groups that are too close to the alkene moiety interfere with monolayer formation and yield disordered monolayers.

Introduction

The preparation of monolayers on solid substrates is technologically important and has been studied for many years. Apart from the monolayers prepared by the Langmuir–Blodgett method, much work has been done in the field of self-assembled monolayers of thiols on gold, and on the chemisorption of trichlorosilanes on oxidized silicon. In both cases dense, well-ordered monolayers are obtained. Many different monolayers have been prepared and their structures thoroughly characterized.^{1,2}

A major drawback of almost all of these monolayers is their low stability. Monolayers of thiols on gold can be quite easily removed when heated in solvents.³ Trichlorosilane-derived layers show good stability, but the silicon–oxygen bonds that are formed are susceptible toward hydrolysis and are thermally labile.⁴ Furthermore, the reproducibility of the synthesis of monolayers by this method is sometimes problematic as well.

Recently, the preparation of dense alkyl monolayers that are covalently bonded to the silicon surface has been reported.^{5,6} It was shown that neat 1-alkenes react efficiently with a hydrogen-terminated silicon(111) surface when heated to 200 °C. This hydrosilylation reaction



Figure 1. Schematic representation of the reaction of 1-alkenes with a hydrogen-terminated silicon surface.

(Figure 1) results in the formation of very stable silicon–carbon bonds,⁷ which yields dense monolayers as evidenced from infrared spectroscopy, ellipsometry, and wetting experiments. These monolayers are at least as stable as similar monolayers on oxidized silicon, as shown in the case of several 1-alkenes and one ω -chloro-1-alkene. The thermal stability up to 615 K of the monolayers in ultrahigh vacuum has very recently been demonstrated.⁸

In this paper, the preparation of highly stable monolayers on the hydrogen-terminated silicon(100) surface is reported, using a variety of both functionalized and nonfunctionalized 1-alkenes. The preparation of functionalized monolayers has been extensively explored for thiols on gold and trichlorosilanes on silicon oxide.^{1,2} However, in contrast to thiols and trichlorosilanes, many functionalized alkenes are readily available or can be easily synthesized. This makes this new reaction, in combination with the stability of the resulting monolayers, potentially very interesting for many applications, e.g., in nonlinear optics⁹ and adsorption experiments.¹⁰ As nonfunctionalized 1-alkenes, 1-octadecene (**I**), 1-hexadecene (**II**), and

* To whom correspondence should be addressed.

[†] Wageningen University.

[‡] FOM–Institute for Atomic and Molecular Physics.

[§] Present address: Koc University, Chemistry Department, Cayir Cad., Istinye 80860 Istanbul, Turkey.

^{||} Utrecht University.

[⊥] Rohm and Haas Company.

(1) Ulman, A. *Chem. Rev. (Washington, D.C.)* **1996**, *96*, 1533–1554.

(2) Ulman, A. *An Introduction to Ultrathin Organic Films*; Academic Press: Boston, MA, 1991.

(3) Tillman, N.; Ulman, A.; Penner, T. L. *Langmuir* **1989**, *5*, 101–111.

(4) Calistri-Yeh, M.; Kramer, E. J.; Sharma, R.; Zhao, W.; Rafailovich, M. H.; Sokolov, J.; Brock, J. D. *Langmuir* **1996**, *12*, 2747–2755.

(5) Linford, M. R.; Chidsey, C. E. D. *J. Am. Chem. Soc.* **1993**, *115*, 12631–12632.

(6) Linford, M. R.; Fenter, P.; Eisenberger, P. M.; Chidsey, C. E. D. *J. Am. Chem. Soc.* **1995**, *117*, 3145–3155.

(7) Terry, J.; Linford, M. R.; Wigren, C.; Cao, R.; Pianetta, P.; Chidsey, C. E. D. *Appl. Phys. Lett.* **1997**, *71*, 1056–1058.

(8) Sung, M. M.; Kluth, G. J.; Yauw, O. W.; Maboudian, R. *Langmuir* **1997**, *13*, 6164–6168.

(9) For some recent examples see: (a) Roscoe, S. B.; Kakkar, A. K.; Marks, T. J.; Malik, A.; Durbin, M. K.; Lin, W.; Wong, G. K.; Dutta, P. *Langmuir* **1996**, *12*, 4218–4223. (b) Collins, T. J.; Tae Bae, I.; Scherson, D. A.; Sukenik, C. N. *Langmuir* **1996**, *12*, 5509–5511. (c) Roscoe, S. B.; Yitzchaik, S.; Kakkar, A. K.; Marks, T. J.; Xu, Z.; Zhang, T.; Lin, W.; Wong, G. K. *Langmuir* **1996**, *12*, 5338–5349. (d) Lin, W.; Lee, T.-L.; Lyman, P. F.; Lee, J.; Bedzyk, M. J.; Marks, T. J. *J. Am. Chem. Soc.* **1997**, *119*, 2205–2211.

1-dodecene (**III**) were used to study the dependence of the alkane chain length on the monolayer formation. To obtain information about the possibility of further functionalization of the thus formed monolayers, ω -ester functionalized 1-alkenes were chosen, since the widespread use of ester groups as protecting groups in organic chemistry and their expected—and observed—unreactivity toward the hydrogen-terminated silicon surface. The unprotected ω -undecenoic acid ($\text{CH}_2=\text{CH}-\text{C}_8\text{H}_{16}-\text{COOH}$, **IV**) and ω -undecenyl alcohol ($\text{CH}_2=\text{CH}-\text{C}_8\text{H}_{16}-\text{CH}_2\text{OH}$, **V**) were employed to study the effects of the presence of two potentially reactive groups in one molecule. The effects of protection of the alcohol and carboxylic acid functionality via ester formation were studied using ω -ester-functionalized 1-alkenes. ω -Undecenyl derivatives $\text{CH}_2=\text{CH}-\text{C}_8\text{H}_{16}-\text{C}(\text{O})\text{O}-\text{CH}_3$ (**VI**), $\text{CH}_2=\text{CH}-\text{C}_8\text{H}_{16}-\text{C}(\text{O})\text{O}-\text{C}_3\text{H}_7$ (**VII**), and $\text{CH}_2=\text{CH}-\text{C}_8\text{H}_{16}-\text{CH}_2\text{O}-\text{C}(\text{O})\text{CH}_3$ (**VIII**) were used to study the effect of ester functionalities far from the reactive alkene moiety, while allyl esters $\text{CH}_2=\text{CH}-\text{CH}_2-\text{O}(\text{O})\text{C}-\text{C}_{11}\text{H}_{23}$ (**IX**) and $\text{CH}_2=\text{CH}-\text{CH}_2-\text{O}(\text{O})\text{C}-\text{C}_{17}\text{H}_{35}$ (**X**) were used to investigate the effect of the sterically demanding ester group close to the reactive site.

Experimental Section

General Information. All chemicals, unless noted otherwise, were commercially available and used as received. Solvents for substrate cleaning were distilled. 1-Octadecene, 1-hexadecene, 10-undecylenic acid, and lauroyl chloride (98%) were obtained from Acros Organics; 1-dodecene, 10-undecen-1-ol, and stearic acid (95%) were obtained from Aldrich. All alkenes for monolayer preparation were distilled at reduced pressure and stored at +4 or -20°C until used. The silicon substrates were either pieces of double-polished silicon (Si(100), n- or p-type, 250 μm thickness), shards of single-polished silicon (Si(100), n- or p-type, 500 μm thickness), or Si(100) parallelogram plates (ATR-plates) designed for multiple internal reflection spectroscopy (Harrick Scientific, 45°, 50 \times 10 \times 1 mm³, 50 reflections).

¹H NMR spectra were recorded in CDCl_3 at 200 MHz on a Bruker AC200 FT-NMR spectrometer at ambient temperature. ¹³C NMR spectra were measured in CDCl_3 at 50 MHz. To obtain more reliable integrations of the ¹³C NMR signals for the compounds **IX** and **X**, pulse sequences with a longer relaxation time, T_1 (up to 20 s), were used. Chemical shifts are in ppm relative to tetramethylsilane. Infrared spectra (IR) of the synthesized alkenes were recorded on a Biorad FTS-7 infrared spectrometer. All liquids were measured between NaCl windows; solids were dissolved in CCl_4 . Melting points were determined on a Mettler FP80 HT melting point apparatus. The measurement conditions for the investigation of the monolayers are described below.

Syntheses: 10-Undecylenic Acid Methyl Ester. A mixture of 10-undecylenic acid (15 g, 81 mmol), 35 mL of methanol, and 0.2 mL of sulfuric acid was refluxed for 3 h. The methanol was removed in vacuo, and the resulting material was dissolved in ether. The organic layer was washed with a sodium bicarbonate solution (2 \times), water (2 \times), and brine. Drying over magnesium sulfate and concentrating yielded 15.5 g of the crude ester as a yellow oil. Vacuum distillation yielded 13.2 g (67 mmol, 82%) of pure (>99%, GC analysis) 10-undecylenic acid methyl ester (bp 115 $^\circ\text{C}$, 11 mmHg).¹¹

¹H NMR: δ 5.90–5.70 (m, 1H), 5.04–4.89 (m, 2H), 3.67 (s, 3H), 2.30 (t, $J = 7.5$ Hz, 2H), 2.09–1.98 (m, 2H), 1.66–1.57 (m, 2H), 1.40–1.23 (m, 10H). ¹³C NMR: δ 174.10, 138.98, 114.03,

51.25, 33.97, 33.68, 29.18, 29.10, 29.03, 28.95, 28.80, 24.84. IR (cm^{-1}): 3075 (m); 2925 (m); 2853 (m); 1740 (s); 1638 (m).

10-Undecylenic Acid Propyl Ester. A mixture of 10-undecylenic acid (15 g, 81 mmol), 1-propanol (7 g, 0.11 mol), and 3 drops of sulfuric acid in 60 mL of toluene was heated in a Dean–Stark setup for 2 h. The toluene was removed in vacuo and the resulting material dissolved in ether. Workup similar to that used for the methyl ester yielded 18.9 g of the crude ester as a brown oil. Vacuum distillation yielded 15.7 g (69 mmol, 85%) of 10-undecylenic acid propyl ester (bp 137–138 $^\circ\text{C}$, 12 mmHg; lit. 139.5 $^\circ\text{C}$ at 7 mmHg).¹²

¹H NMR: δ 5.90–5.70 (m, 1H), 5.04–4.88 (m, 2H), 4.01 (t, 2H, $J = 6.7$ Hz), 2.29 (t, 2H, $J = 7.4$ Hz), 2.08–1.97 (m, 2H), 1.72–1.55 (m, 4H), 1.41–1.25 (m, 10H), 0.93 (t, 3H, $J = 7.4$ Hz). ¹³C NMR: δ 174.22, 139.42, 114.48, 66.12, 34.97, 34.14, 29.65, 29.57, 29.28, 29.41, 29.25, 25.36, 22.37, 10.73. IR (cm^{-1}): 3077 (m); 2967 (m); 2928 (m); 2855 (m); 1738 (s); 1640 (m).

10-Undecylenyl Acetate. A mixture of 10-undecylenyl alcohol (12 g, 70 mmol) and acetic acid anhydride (8 mL, 85 mmol) was refluxed for 1 h. The resulting liquid was poured onto 50 mL of ice water. The organic layer was separated and the water layer extracted with 50 mL of ether. The organic layers were combined and washed with a sodium bicarbonate solution (2 \times), water (2 \times), and brine. Drying over magnesium sulfate and concentration yielded 14.0 g of product as a yellow oil. Distillation yielded 11.8 g (56 mmol, 79%) of 10-undecylenyl acetate (bp 128–129 $^\circ\text{C}$, 11 mmHg; lit. 125–127 $^\circ\text{C}$ at 7 mmHg).¹³

¹H NMR: δ 5.93–5.70 (m, 1H), 5.03–4.89 (m, 2H), 4.04 (t, 2H, $J = 6.7$ Hz), 2.03 (s, 3H), 2.05–1.98 (m, 2H), 1.65–1.56 (m, 2H), 1.40–1.22 (m, 12H). ¹³C NMR: δ 171.09, 139.07, 114.05, 64.55, 33.73, 29.38, 29.32, 29.16, 29.02, 28.84, 28.54, 25.84, 20.90. IR (cm^{-1}): 3076 (w); 2927 (m); 2855 (m); 1743 (s); 1640 (m).

Allyl Dodecanoate. Lauroyl chloride (23.1 mL, 0.10 mol) was added dropwise with stirring to 10 mL of allyl alcohol at 0 $^\circ\text{C}$. The resulting mixture was stirred for 1 h, allowing it to warm to room temperature. The solution was poured onto 100 mL of water. Extraction with 50 mL of petroleum ether 40–60 $^\circ\text{C}$ yielded an organic layer which was subsequently washed with a sodium bicarbonate solution and brine. The combined water layers were made alkaline and extracted with a small portion of petroleum ether. The organic layers were combined and dried over magnesium sulfate. Concentration yielded 25.6 g of crude allyl dodecanoate as a yellow oil. Distillation yielded 20.4 g (85 mmol, 85%) of the pure ester (bp 149–150 $^\circ\text{C}$, 10 mmHg; lit. 162–164 $^\circ\text{C}$ at 20 mmHg).¹⁴

¹H NMR: δ 6.02–5.83 (m, 1H), 5.37–5.20 (m, 2H), 4.58 (dt, 2H, $J = 5.7$ Hz, $J = 1.4$ Hz (2 \times)), 2.33 (t, 2H, $J = 7.5$ Hz), 1.71–1.56 (m, 2H), 1.32–1.22 (m, 16H), 0.88 (t, 3H, $J = 6.8$ Hz). ¹³C NMR: δ 173.27, 132.35, 117.84, 64.79, 34.17, 31.87, 29.56 (2 C), 29.41, 29.30, 29.22, 29.10, 24.90, 22.63, 14.02. IR (cm^{-1}): 3085 (w); 2925 (m); 2854 (m); 1741 (s); 1649 (m).

Allyl Octadecanoate. A mixture of stearic acid (20 g, 70 mmol), allyl alcohol (6 g, 0.10 mol), and 3 drops of sulfuric acid in 60 mL of toluene was heated in a Dean–Stark setup for 2 h. The toluene was removed in vacuo, and the resulting oil poured onto 150 mL of a 10% NaCl solution. The water layer was subsequently extracted with 50 mL of ether and 50 mL of petroleum ether (40–60 $^\circ\text{C}$). The organic layers were combined, washed with brine, and dried over magnesium sulfate. The solvent was removed, yielding 23.4 g of crude product as a yellow, waxlike material. This was dissolved in 200 mL of 96% ethanol

(11) (a) The literature value for 10-undecylenic acid methyl ester is 124 $^\circ\text{C}$ at 10 mmHg,^{11a} a suspicious value when compared to the ethyl ester, which has 131.5 $^\circ\text{C}$ at 16 mmHg.^{11b} The methyl ester has been prepared several times and displayed a bp between 113 $^\circ\text{C}$ (10 mmHg) and 116 $^\circ\text{C}$ (12 mmHg) in all cases, which was not affected by repeated distillation. Because no impurities could be found upon GC-analysis, it is assumed that the literature value is incorrect. (b) *Handbook of Chemistry and Physics*, 52nd ed.; The Chemical Rubber Co.: Cleveland, OH, 1971.

(12) *Beilstein Handbook of Organic Chemistry*, 4th ed. (abbreviated as Beilstein); Springer-Verlag: Berlin, Germany, Vol. 2, supplementary series III, p 1364. This ester shows the same large difference in boiling points as the methyl ester, but again NMR and GC-analysis showed no impurities.

(13) Beilstein, Vol. 2, supplementary series II, p 152.

(14) Beilstein, Vol. 2, supplementary series III, p 887.

(10) For some recent examples see: (a) Fragneto, G.; Lu, J. R.; McDermott, D. C.; Thomas, R. K.; Rennie, A. R.; Gallagher, P. D.; Satija, S. K. *Langmuir* **1996**, *12*, 477–486. (b) Madoz, J.; Kuznetsov, B. A.; Medrano, F. J.; Garcia, J. L.; Fernandez, V. M. *J. Am. Chem. Soc.* **1997**, *119*, 1043–1051. (c) Heise, A.; Menzel, H.; Yim, H.; Foster, M. D.; Wieringa, R. H.; Schouten, A. J.; Erb, V.; Stamm, M. *Langmuir* **1997**, *13*, 723–728. (d) Silin, V.; Weetall, H.; Vanderah, D. J. *J. Colloid. Interface Sci.* **1997**, *185*, 94–103. (e) Petrash, S.; Sheller, N. B.; Dando, W.; Foster, M. D. *Langmuir* **1997**, *13*, 1881–1883.

at 60 °C and crystallized via slow cooling to 0 °C. The product was filtered, washed with a small amount of cold ethanol, and thoroughly dried in vacuo at room temperature, yielding 14.8 g (46 mmol, 65%) of allyl stearate (mp 34.5–35 °C; lit. 35 °C).¹⁵ A further 3.4 g of product was isolated from the filtrate by removal of the ethanol and recrystallizing the resulting material from 40 mL of 96% ethanol following the same procedure.

¹H NMR: δ 6.03–5.80 (m, 1H), 5.36–5.20 (m, 2H), 4.58 (dt, 2H, $J = 5.7$ Hz, $J = 1.4$ Hz (2 \times)), 2.33 (t, 2H, $J = 7.5$ Hz), 1.70–1.56 (m, 2H), 1.38–1.20 (m, 28H), 0.88 (t, 3H, $J = 6.5$ Hz). ¹³C NMR: δ 173.34, 132.36, 117.90, 64.83, 34.22, 31.92, 29.69 (large signal, 6 C), 29.59, 29.45, 29.36, 29.25, 29.14, 24.93, 22.67, 14.06. IR (cm⁻¹): 3087 (w); 2926 (m); 2854 (m); 1740 (s); 1647 (m).

Monolayer Preparation. Approximately 2 mL of the distilled alkene was placed in a small glass tube and deoxygenated with dry nitrogen for at least 30 min. A piece of silicon was etched for 1 min in 2% hydrofluoric acid, blown dry with nitrogen, and immediately placed in the deoxygenated alkene. The tube was then placed in an oil bath of 200 °C for 2 h, while slowly bubbling nitrogen through the alkene. Subsequently, the silicon piece was removed from the solution, rinsed 3 times in petroleum ether (40–60 °C) and ethanol (96%), sonicated for 5 min in dichloromethane, and dried in a stream of nitrogen. For the 10-undecenyl ester-derived monolayers, methanol or propanol was used instead of ethanol.

For large samples such as attenuated total reflectance (ATR)-crystals, a flattened glass tube with a screw cap was used, which was filled with sufficient alkene to completely immerse the silicon substrate. The alkene was deoxygenated with nitrogen for at least 1 h. These samples were cleaned in boiling dichloromethane instead of by sonication. The modified ATR-crystals were cleaned between monolayer preparations by a UV/ozone treatment. The crystal was placed approximately 1 cm from the lamp and each side was illuminated for 10–15 min.^{16,17} After this oxidation, drops of water completely spreaded on the silicon substrate, showing the complete removal of the monolayer. The crystals were subsequently etched in HF prior to renewed use.

Stability tests and modifications of the monolayers were performed in a small flask or, in the case of the ATR-crystals, in a large glass tube (50 mL) with a reflux condenser. For the acidification of solvents, a few drops of sulfuric acid were used.

Contact Angle Measurements. Water contact angles were measured with a KSV Sigma 701 tensiometer, using a computer-controlled contact angle calculation program, available from the manufacturer. The silicon sample (double polished, approximately 15 \times 7 mm², thickness 250 μ m) was placed vertically in a counterbalanced, homemade clamp and used as a Wilhelmy-plate. This method is often used for the determination of static contact angles but can be used for dynamic contact angles as well.¹⁸ For both advancing and receding contact angles at least six measurements were made. For the monolayers of **I–VIII** the reproducibility for advancing contact angles is $\pm 1^\circ$ and for the receding angles ± 1 – 2° . For the monolayers of **IX** and **X** the experimental errors are estimated to be $\pm 3^\circ$.

Infrared Spectroscopy. Infrared spectra of the monolayers were recorded on a Perkin-Elmer 2000 FT-IR spectrometer, equipped with a liquid-nitrogen-cooled MCT-detector, using a fixed angle multiple reflection attachment (Harrick Scientific). The infrared light was incident on one of the 45° levels of the ATR-plate. Spectra of the monolayers were recorded with s- and p-polarized light. Measurement conditions were as follows: resolution 4 cm⁻¹, at least 256 scans, apodization medium Norton-Beer. The spectra were measured in the range of 4000–1500 cm⁻¹, following from the high absorbance of silicon ATR-crystals below 1500 cm⁻¹. An ATR-crystal was cleaned with ethanol and chloroform and used as a background. No corrections were made for water vapor or CO₂. In some cases a linear baseline correction or a fringe correction was applied.¹⁹ To remove physisorbed material, the samples were rinsed extensively in chloroform before mounting.

The reproducibility of the peak positions in different measurements, e.g., after repositioning of the sample or cleaning of the monolayer-modified crystal, was within 0.5 cm⁻¹. The use of a freshly etched and cleaned silicon background crystal instead of the oxidized surface gave no improvement.

From the measurement of the independent s- and p-polarized spectra the dichroic ratio $D = A_s/A_p$ can be calculated, in which A is the intensity of the absorbance measured with s- or p-polarized light.²⁰ The determination of D allows for an estimate of the angle α between the transition dipole moment of the vibration and the surface normal²¹

$$\alpha = \tan^{-1} \left[\frac{2DE_z^2}{E_y^2 - DE_x^2} \right]^{1/2}$$

in which $E_{x,y,z}$ are the electric fields of the polarized light for the x , y , and z directions, respectively.²² For the ATR conditions in our experiments $E_x = 1.409$, $E_y = 1.476$, and $E_z = 0.684$, using refractive indices of $n_{\text{Si}} = 3.5$ and $n_{\text{monolayer}} = 1.5$.²¹ From the determination of α for both the antisymmetric (α_a) and symmetric (α_s) methylene stretching vibrations, an estimated tilt angle, Φ_{tilt} , of the molecule, with respect to the surface normal can be calculated using

$$\cos^2 \Phi_{\text{tilt}} = 1 - \cos^2 \alpha_s - \cos^2 \alpha_a$$

X-ray Reflectivity. X-ray reflectivity measurements were performed using a rotating anode Rigaku RU-300H generator having a maximum power of 18 kW and a triple-axis reflectometer. This setup has been described in detail previously.²⁴ The incident beam (Cu K α radiation, $\lambda = 1.5405$ Å) was monochromatized and focused using a bent graphite (002) crystal. The incident and outgoing divergences, as defined by the slit widths, were 0.064° and 0.082°, respectively, corresponding to in-plane resolutions of $\Delta q_z = 7.4 \times 10^{-3}$ Å⁻¹ and $\Delta q_x = 3.2 \times 10^{-3}$ Å⁻¹. Samples were mounted on a substrate holder and measured in ambient air. No sign of beam damage or contamination was observed. The 10-undecenyl alcohol-derived monolayer (**V**) was rinsed in acetic acid and water prior to measurement and measured in a cell that was vacuum-pumped continuously to avoid contamination through air exposure.

X-ray reflectivity data are background subtracted, and standard geometrical correction for the beam footprint has been applied. The alkyl monolayers were modeled as having a constant electron density throughout the film. For the end-group-functionalized monolayers a three-layer model was used. The root mean square roughness of the air/film and film/substrate interfaces was described by a Gaussian function. Fits were calculated with an iterative matrix solution of the Fresnel equations for the reflectivity of the air/film/substrate system, using periodic slab profiles of electron densities.²⁴

Results and Discussion

Monolayer Properties: Ordering and Packing Structures. The monolayers were analyzed by contact angle measurements, multiple internal reflection infrared spectroscopy, and X-ray reflectivity (vide infra). A combination of the results obtained from these measurements provides information on the ordering and packing of the

(19) The fringes that appear in the infrared spectra are due to minor variations between the position and the size of the ATR-samples and the background. It is possible to remove these fringes by applying a mathematical correction on the obtained interferogram. The band positions are not affected, but the intensities of the bands are lowered. The correction was only applied to the carbonyl stretching region. Nissink, J. W. M. Unpublished results.

(20) Tillman, N.; Ulman, A.; Schildkraut, J. S.; Penner, T. L. *J. Am. Chem. Soc.* **1988**, *110*, 6136–6144.

(21) Linford, M. R. Ph.D. Thesis, Stanford University, Stanford, CA, June 1996.

(22) Haller, G. L.; Rice, R. W. *J. Phys. Chem.* **1970**, *74*, 4386–4393.

(23) Higashiyama, T.; Takenaka, T. *J. Phys. Chem.* **1974**, *78*, 941–947.

(24) Mol, E. A. L.; Schindler, J. D.; Shalaginov, A. N.; de Jeu, W. H. *Phys. Rev. E* **1996**, *54*, 536.

(15) Beilstein, Vol. 2, supplementary series III, p 1019.

(16) Frantz P.; Granick, S. *Langmuir* **1992**, *8*, 1176–1182.

(17) Brunner, H.; Vallant, T.; Mayer U.; Hoffmann, H. *Langmuir* **1996**, *12*, 4614–4617.

(18) Ramé, E. *J. Colloid Interface Sci.* **1997**, *185*, 245–251 (erratum see 189, 383).

Table 1. Water Contact Angles and Infrared Absorptions (in cm^{-1}) for the Antisymmetric (ν_a) and Symmetric (ν_s) Methylene Stretching Vibrations of the Monolayers

alkene	$\Theta_{a/r}$ (H_2O) ^a (deg)	ν_a	ν_s
$\text{CH}_2=\text{CH}-\text{C}_{16}\text{H}_{33}$ (I)	110/96	2920	2851
$\text{CH}_2=\text{CH}-\text{C}_{14}\text{H}_{29}$ (II)	109/95	2921	2852
$\text{CH}_2=\text{CH}-\text{C}_{10}\text{H}_{21}$ (III)	109/94	2920 ^b	2849 ^b
$\text{CH}_2=\text{CH}-\text{C}_8\text{H}_{16}-\text{COOH}$ (IV)	0 ^c	2925	2854
$\text{CH}_2=\text{CH}-\text{C}_8\text{H}_{16}-\text{CH}_2\text{OH}$ (V)	0 ^c	2923	2853
$\text{CH}_2=\text{CH}-\text{C}_8\text{H}_{16}-\text{COO}-\text{CH}_3$ (VI)	77/70	2923	2854
$\text{CH}_2=\text{CH}-\text{C}_8\text{H}_{16}-\text{COO}-\text{C}_3\text{H}_7$ (VII)	85/73	2920	2850
$\text{CH}_2=\text{CH}-\text{C}_8\text{H}_{16}-\text{CH}_2\text{O}-\text{C}(\text{O})\text{CH}_3$ (VIII)	73/65	2919	2850
$\text{CH}_2=\text{CH}-\text{CH}_2-\text{OOC}-\text{C}_{11}\text{H}_{23}$ (IX)	101/89	2925	2856
$\text{CH}_2=\text{CH}-\text{CH}_2-\text{OOC}-\text{C}_{17}\text{H}_{35}$ (X)	106/91	2923	2854

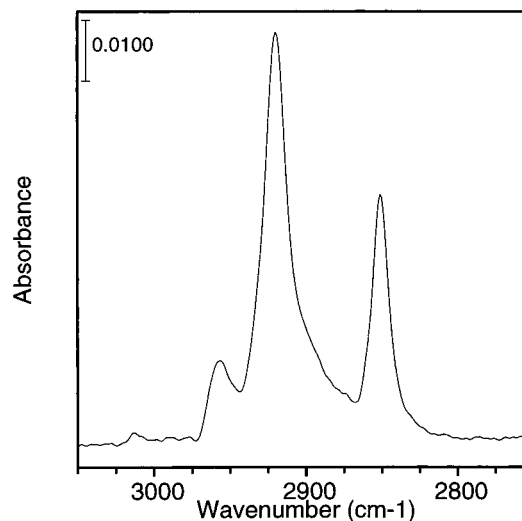
^a Advancing and receding contact angles for water. ^b Maximum shifted to lower value due to low absorption and subsequent problems with negative peaks as a result of background contamination. ^c Directly after cleaning of the substrate in acetic acid and water, a small drop of water tends to spread on the surface. However, these contact angles are not stable in time.^{3,26,34}

monolayers. The water contact angles, as observed for the monolayers on Si(100), are listed in Table 1 (column 2). This table also contains the infrared peak positions, as observed with p-polarized light, for the antisymmetric (ν_a) and symmetric (ν_s) methylene stretching vibrations (columns 3 and 4, respectively).

The measurement of water contact angles is a quick and useful tool in monolayer analysis.²⁵ It can also be used to study the monolayer stability, if measured as a function of time, as monolayers that are disordered or not stable will show decreasing contact angles. No such changes were observed for any of the monolayers listed in Table 1.

From the high values of the water contact angles ($\Theta_{a/r} = 109-110^\circ/94-96^\circ$) as measured for the unfunctionalized 1-alkenes (**I-III**), it is clear that the surface of the monolayer is completely terminated by methyl groups. The advancing contact angles are comparable to those of thiols on gold,^{26,27} and for the monolayers on silicon (111) prepared by Linford et al.⁶ This shows that a sufficiently high percentage of the hydrogenated silicon atoms has reacted with a 1-alkene to give a complete coverage of the surface. The surface properties of the monolayer are therefore not affected by residual Si-H and Si-OH groups that are present on the silicon surface.⁶ The receding contact angles are somewhat lower than the reported literature values as a result of surface roughness, which leads to an increase in the contact angle hysteresis $\Delta\Theta$ (defined as $\Delta\Theta = \Theta_a - \Theta_r$).²⁸ However, the comparatively large hysteresis may also be the result of a slightly higher number of defects in the monolayers when compared to the trichlorosilane monolayers.

Infrared spectroscopy reveals that for the samples **I-III** the antisymmetric and symmetric methylene stretching vibrations appear near 2920 and 2850 cm^{-1} , respectively (Table 1). It is well-known that shifts from 2928 to 2920 cm^{-1} and from 2856 to 2850 cm^{-1} for the methylene stretching vibrations occur on going from a liquid to a solid alkane.²⁹ The observed wavenumbers are therefore indicative of a densely packed monolayer of alkyl chains.³⁰ The IR-spectrum of the monolayer of **I** is shown in Figure 2.

**Figure 2.** Infrared spectrum (C-H stretching region) of a monolayer of **I** on Si(100).

The contact angles, as observed for the functionalized monolayers of **IV-VIII**, do not provide conclusive information in all cases. The acid- and alcohol-terminated monolayers (samples **IV** and **V**, respectively) show very low contact angles. This is expected for a surface terminated by hydrophilic groups, but might also be due to a disordered surface. Unfortunately, contact angle measurements cannot resolve this matter. For a methyl ester-terminated surface, different values are reported for thiols on gold ($\Theta_a = 67^\circ$ ²⁶) and trichlorosilanes on silicon oxide ($\Theta_a = 72^\circ-79^\circ$ ³¹). The advancing contact angle as observed for the monolayer of **VI** ($\Theta_a = 77^\circ$) is comparable to these values and indicates that the surface is terminated with methyl ester groups. The small hysteresis ($\Delta\Theta = 7^\circ$) suggests that the methyl groups are close together and a closely packed monolayer is formed. A similarly small hysteresis ($\Delta\Theta = 8^\circ$) is observed for the acetate-terminated surface (**VIII**), which shows $\Theta_{a/r} = 73/65^\circ$. These values are comparable to the recently published data ($\Theta_{a/r} = 64/58^\circ$) for an acetate-terminated monolayer on gold.³² The monolayers of both **VI** and **VIII** show contact angles that are slightly higher than those on gold. This is probably caused by the surface roughness of the silicon substrate, which will expose some underlying CH_2 groups. As this moiety has a low dipole moment and polarizability, this extra exposure will result in an increased hydrophobicity. The observed advancing contact angle for the propyl ester surface **VII** ($\Theta_a = 85^\circ$) shows that the hydrophobicity increases as the ester group gets buried in the monolayer. This value gets closer to the values observed for the long alkyl chains **I-III**, which confirms that the ester groups in the monolayers of **VI-VIII** are at the air/monolayer interface.

The infrared data of samples **VI**, **VII**, and **VIII** show that well-ordered monolayers are obtained if the functional end groups are protected as ester moieties. Monolayers of **VII** and **VIII** show absorption maxima that indicate very closely packed molecules. Apparently, the ester groups are not too big and still allow for dense packing of the monolayer. The observed maxima for the monolayer of **VI** are somewhat higher, in line with the reported

(25) Ulman, A., ref 2, p 253.

(26) Bain, C. D.; Troughton, E. B.; Tao, Y.-T.; Evall, J.; Whitesides, G. M.; Nuzzo, R. G. *J. Am. Chem. Soc.* **1989**, *111*, 321-335.(27) Bain, C. D.; Evall, J.; Whitesides, G. M. *J. Am. Chem. Soc.* **1989**, *111*, 7155-7164.

(28) Ulman, A., ref 2, p 53, and references therein.

(29) Snyder, R. G.; Strauss, H. L.; Elliger, C. A. *J. Phys. Chem.* **1982**, *86*, 5145-5150.(30) Porter, M. D.; Bright, T. B.; Allara, D. L.; Chidsey, C. E. D. *J. Am. Chem. Soc.* **1987**, *109*, 3559-3568.(31) Pomerantz, M.; Segmüller, A.; Netzer, L.; Sagiv, J. *Thin Solid Films* **1985**, *132*, 153-162.(32) Engquist, I.; Lestelius, M.; Liedberg, B. *Langmuir* **1997**, *13*, 4003-4012.

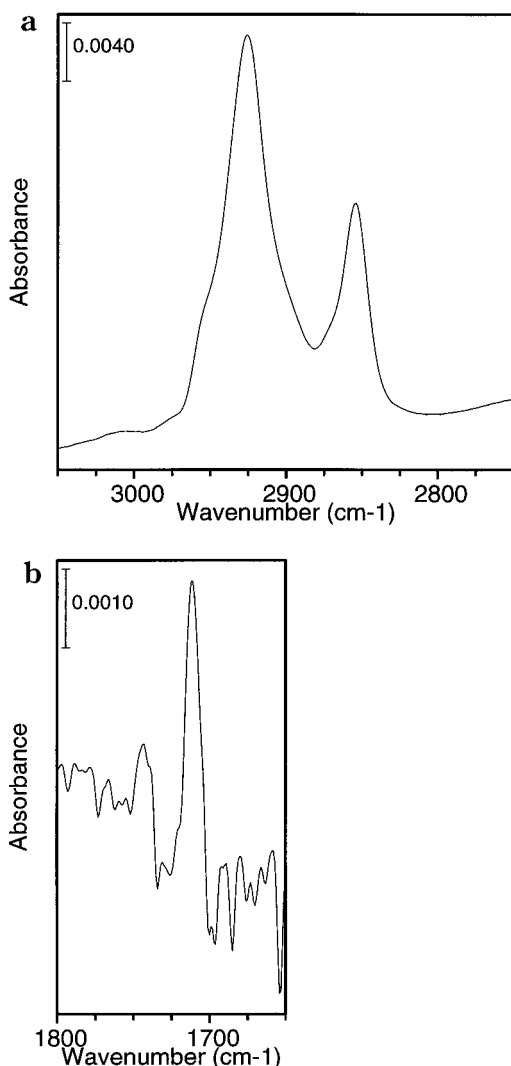


Figure 3. Infrared spectra (C-H and C=O stretching regions) of a monolayer of **IV** on Si(100): (a) C-H stretching region; (b) C=O stretching region.

observation that methylene stretching frequencies shift to higher values as the alkyl chains in alkyl monolayers get shorter and suffer from gauche defects, but a close packing is also obtained with this protecting group.^{31,33}

The unprotected undecylenic acid (**IV**) seems to give a quite disordered surface. In the infrared spectrum of the monolayer (Figure 3) the methylene stretching vibrations appear as somewhat broadened peaks with maxima at 2925 and 2854 cm^{-1} , which indicates that the monolayer is not as well-ordered as the alkyl monolayers of **I-III**. The shift of the absorption maximum to a higher frequency is the result of gauche conformations, which are possible if the molecules in the monolayer are not close together. However, a similar shift is observed when an originally ordered monolayer reorganizes, e.g., by a folding of the alkyl chains to remove the polar headgroups from the outside of the surface.³⁴ In the carbonyl-stretching region two peaks are observed: one at 1711 cm^{-1} , which can be attributed to the normal, hydrogen-bonded C=O vibration of carboxylic acid dimers, and one at 1740 cm^{-1} , corresponding to the carbonyl stretching vibration of a free

carboxylic acid.³⁵ On the other hand, if the acid group is bound to the silicon surface, the C=O vibration of the resulting Si-O-C=O ester is at $\sim 1710 \text{ cm}^{-1}$ as well.^{5,6,36,37} The latter situation did, however, not seem to occur, as no terminal alkene vibrations were observed in the IR spectrum.

To further investigate this surface, it was reacted with boiling acidic methanol for 20 min to hydrolyze any siloxane esters present and to introduce the methyl ester functionality. The resulting removal of any molecules from the monolayer will yield a shift of the vibrational frequencies of the methylene groups to higher wavenumbers, as observable by IR spectroscopy. After the reaction, the C=O vibration at 1710 cm^{-1} had disappeared and a broad peak at 1743 cm^{-1} showed the presence of terminal methyl ester groups. The maximum of the antisymmetric methylene absorption had shifted to 2928 cm^{-1} , was considerably broadened, and had decreased about 40% in intensity. These observations indicate that siloxane esters are formed in the reaction of the bifunctional alkene **IV** with the hydrogen-terminated silicon surface and that the peak at 1710 cm^{-1} must arise, at least partially, from these siloxane esters that are apparently formed by a reaction of the carboxylic acid moiety with this surface. Consequently, a disordered monolayer is obtained, instead of an acid-terminated monolayer that reorganizes in time. The reaction of organic acids with a hydrogen-terminated silicon surface has been reported in the literature, but only under the influence of light^{36,37} or with an applied bias.³⁸ The reaction with a clean, oxide-free silicon surface has been reported as well.³⁹ Our results suggest that this also occurs at high temperatures, although a reaction with either defects or silanol groups at the surface cannot be fully excluded.

The unprotected alcohol **V** showed broad bands with maxima at 2923 and 2853 cm^{-1} , which is indicative of a disordered monolayer. Alcohols can react with a hydrogen-terminated silicon surface at elevated temperatures,^{40,41} but as the quality of the infrared spectrum obtained was very poor, no reliable conclusion about the presence of any terminal alkene groups could be drawn. Upon treatment of this surface with acetic anhydride, a small peak around 1740 cm^{-1} was observed, and the absorption maximum of the CH_2 stretching vibration appeared at 2925 cm^{-1} . The peak at 1740 cm^{-1} is assigned to the formation of ester groups, which shows that alcohol groups were still present in the monolayer. However, if an ordered, but reorganized,³⁴ hydroxyl-terminated monolayer had been formed on the surface, a shift of the methylene stretching vibrations to a lower wavenumber is expected, because the resulting monolayer, after reaction with acetic anhydride, should be comparable to the acetate-terminated surface **VIII**.

To investigate the reactivity of an alcohol group toward the hydrogen-terminated surface under our experimental conditions, the surface was modified with neat dodecanol. After the surface was cleaned in petroleum ether (40–60

(35) Cheng, S. S.; Scherson, D. A.; Sukenik, C. N. *Langmuir* **1995**, *11*, 1190–1195.

(36) Lee, E. J.; Ha, J. S.; Sailor, M. J. *J. Am. Chem. Soc.* **1995**, *117*, 8295–8296.

(37) Lee, E. J.; Bitner, T. W.; Ha, J. S.; Shane, M. J.; Sailor, M. J. *J. Am. Chem. Soc.* **1996**, *118*, 5375–5382.

(38) Green, W. H.; Lee, E. J.; Lauerhaas, J. M.; Bittner, T. W.; Sailor, M. J. *Appl. Phys. Lett.* **1995**, *67*, 1468–1470.

(39) Bitner, T.; Alkunschalie, T.; Richardson, N. V. *Surf. Sci.* **1996**, *368*, 202–207.

(40) Cleland, G.; Horrocks, B. R.; Houlton, A. *J. Chem. Soc., Faraday Trans.* **1995**, *91*, 4001–4003.

(41) Kim, N. Y.; Laibinis, P. E. *J. Am. Chem. Soc.* **1997**, *119*, 2297–2298.

(33) Hostetler, M. J.; Stokes, J. J.; Murray, R. W. *Langmuir* **1996**, *12*, 3604–3612.

(34) Evans, S. D.; Evall, J.; Whitesides, G. M. *J. Am. Chem. Soc.* **1989**, *111*, 7155–7164.

°C) and cold dichloromethane, it did not show hydrophobicity when a drop of water was placed on a slightly tilted sample. The infrared spectrum showed broad absorptions for the methylene stretches with maxima at 2926 and 2854 cm^{-1} . The corresponding monolayer prepared from dodecene (compound **III**) is hydrophobic and has methylene absorption maxima at 2920 and 2850 cm^{-1} (Table 1). This indicates that the alcohol does indeed react with the surface but that a well-packed monolayer is not formed.

The allyl esters **IX** and **X** both give disordered monolayers. The water contact angles are significantly lower than for the alkyl monolayers of **I–III**, suggesting that the surface is not completely methyl-terminated. The infrared data show that the alkyl chains are not as densely packed as the corresponding monolayers from the 1-alkenes **I–III**, since the maxima of the antisymmetric methylene absorptions are observed at slightly higher wavenumbers (2923–2925 cm^{-1} compared to 2920–2921 cm^{-1}). The same difference is observed for the symmetric methylene stretches. It has been reported that an ordered monolayer was obtained for a similar compound on a gold surface, indicating that this class of compounds can give dense monolayers if enough space is available for the ester group.⁴² The steric hindrance of an ester group near the silicon surface apparently hampers the alkene to approach the nearest silicon atom and prohibits formation of a closely packed monolayer on the silicon(100) surface.

Monolayer Properties: Electron Density, Thickness and Roughness. As the ordering and close packing of the monolayers have been established, more detailed information is desirable to further characterize these types of structures, such as the thickness of the layer and the interfacial roughness. This type of data can be obtained via X-ray reflectivity, which is sensitive to changes in the average electron density ρ along the momentum transfer vector Q , which is related to the momentum of the X-ray photons during the reflection process.⁴³ In specular reflectivity, where the angle Θ of the incoming X-ray beam with the surface is equal to the angle of the reflected beam, $Q(\Theta) = (4\pi/\lambda) \sin(\Theta)$ and the vector is perpendicular to the film surface. The reflectivity profile is a function of the momentum transfer $Q(\Theta)$. Below the critical value of momentum transfer Q_c , total reflection is observed; beyond Q_c , the reflectivity follows the Fresnel law for a single sharp interface. Therefore, from deviations from Fresnel reflectivity of the substrate, information about the density profile along the surface normal (i.e., the electron density variation within the monolayer), film thickness, and interface roughnesses of a monolayer can all be derived in one experiment. This makes it a powerful technique for the analysis of thin films on solid substrates. The monolayers of **I–III**, **V**, and **VIII** were studied by X-ray specular reflectivity measurements, and the results reported in Figures 4–6.

Figure 4 shows the X-ray reflectivity as a function of momentum transfer Q for the alkane monolayers of **I–III** on the silicon(100) surface. For all three layers Q_c is 0.028 \AA^{-1} , which corresponds to a critical angle of 0.2°, a typical value for the underlying silicon substrate.⁴⁴ The angle of incidence was increased up to 5°, corresponding to a maximum Q value of 0.7 \AA^{-1} . This allowed for the observation of a second minimum in the reflectivity profile

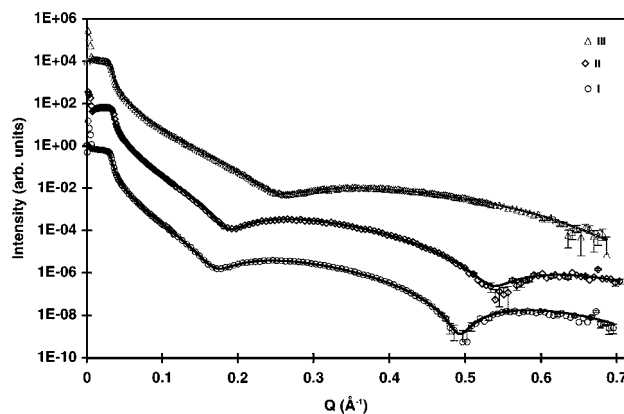


Figure 4. X-ray reflectivity profiles of monolayers of **I–III** on Si(100), also showing best-fit curves and error bars.

Table 2. Various Film Properties as Obtained from Single-Layer Fits to the X-ray Reflectivity Measurements^a

monolayer ^b	thickness (Å)	e density ($\text{e}^{-}/\text{\AA}^3$)	σ_2 (Å) ^c	σ_3 (Å) ^d	tilt angle ^e (deg)
I	19.5	0.32	2.6	2.9	29
I (on Si(111))	19.7	0.30	2.6	4.1	28
II	17.8	0.31	2.5	3.5	26
III	13.2	0.30	1.7	2.7	26
V	17.1 (14.4)	0.52	1.6 (3.8)	1.6 (2.0)	^f
VIII	16.1 (16.4)	0.34	2.5 (2.0)	2.4 (2.9)	17

^a When improved fits are possible using more layers, the results are placed in parentheses. Approximate errors, based on the scatter of values determined from measurements of different samples of monolayers **I**, **II**, and **III**, are as follows: thickness $\pm 1\%$, e density $\pm 3\%$, $\sigma_2 \pm 2\%$, $\sigma_3 \pm 10\%$. ^b Monolayer on silicon (100), unless otherwise specified. ^c Roughness of air/monolayer interface. ^d Roughness of monolayer/silicon interface. ^e Tilt angle as calculated from X-ray reflectivity results. ^f Not determined (see below for explanation).

for the relatively thick samples **I** and **II**, which results in an accurate determination of the film thickness. With increasing film thickness, going from top to bottom in Figure 4, the period of the reflectivity minima decreases and the position of the reflectivity minima shifts to lower Q values. The solid lines in Figure 4 are single layer best fits to the data, as described in the Experimental Section. The electron density of the silicon substrate was fixed at 7.89 $\text{e}^{-}/\text{\AA}^3$ and the mass absorption coefficient at 5.49 $\times 10^{-6} \text{\AA}^{-1}$.

For some data points at large Q values, the error bars due to counting statistics are also shown. It should be noted that the total error is likely to be somewhat larger due to other contributions, such as instrumental misalignment. The measurements cover an intensity range of more than 8 orders of magnitude before the background is reached. It is clear from the relatively large error bars that the second minima observed in monolayers of **I** and **II** are close to the background, leading to increased deviations between the data and the fitted curves in this part of the reflectivity profile. This results in a slight increase of the uncertainty in the monolayer thickness.

The calculated film thickness, electron density, and interface roughnesses of the monolayers of **I–III** are listed in Table 2. For the film thickness a clear linearity is observed, as expected for a series of long alkyl chains. Each methylene group adds approximately 1 Å to the monolayer thickness. The values are consistent with a constant tilt angle of 27° for all three layers, as will be discussed below.

(42) Clegg, R. S.; Hutchison, J. E. *Langmuir* **1996**, *12*, 5239–5243.

(43) For an explanation of X-ray specular reflection analysis of thin layers see e.g.: (a) Wasserman, S. R.; Whitesides, G. M.; Tidswell, I. M.; Ocko, B. M.; Pershan, P. S.; Axe, J. D. *J. Am. Chem. Soc.* **1989**, *111*, 5852–5861. (b) Tidswell, I. M.; Ocko, B. M.; Pershan, P. S.; Wasserman, S. R.; Whitesides, G. M.; Axe, J. D. *Phys. Rev. B* **1990**, *41*, 1111–1128.

(44) Russell, T. *Mater. Sci. Rep.* **1990**, *5*, 171–271.

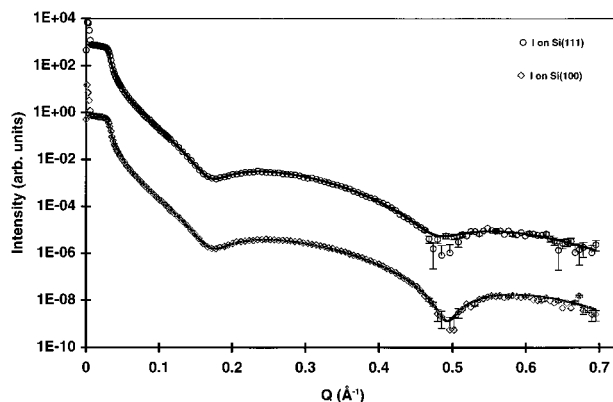


Figure 5. X-ray reflectivity profiles of a monolayer of **I** on Si(111) and Si(100).

The average electron density for all three layers is nearly constant at a value of $0.31 \pm 0.02 \text{ e}^-/\text{\AA}^3$. For comparison, the density of crystalline $\text{C}_{33}\text{H}_{68}$ is $0.35 \text{ e}^-/\text{\AA}^3$,⁴⁵ which again indicates that the alkyl chains in the monolayers of **I–III** are closely packed. The interface roughnesses are 1–4 Å, comparable to the roughness of 2–4 Å usually found for silicon, while the roughness at the air/monolayer interface is smaller than at the monolayer/substrate interface. Apparently the outside of the monolayer can somewhat reorganize and form a smooth outer layer, while at the monolayer–silicon surface, the roughness is determined by the original hydrogen-terminated Si(100) surface. A similar smoothening of the outside of the monolayer has been observed for mono- and multilayers of behenic acid on silicon oxide.⁴⁶

To compare the results on the silicon (100) surface with monolayers on silicon (111), a monolayer of **I** on this latter surface was prepared following a literature procedure.⁶ The similarity of the X-ray specular reflectivity data for the two monolayers can be seen in Figure 5. The solid lines are the best fits to the data and error bars are due to counting statistics. As shown in Table 2, the thicknesses determined from the fits are almost identical, differing by only 1%. The electron densities differ by 7%, which is within the scatter of values obtained from different fits, e.g., when using an optimized or the literature value for the electron density of the silicon substrate.

The similarity of the monolayer of **I** on the silicon (111) and (100) surface is not unexpected. The two hydrogen-terminated surfaces are different, but from a simple ball-and-stick model, it is clear that on both surfaces only 50% of the hydrogenated silicon atoms can react with an alkene due to steric hindrance, as was already suggested by Linford et al. for their monolayers on the silicon (111) surface.⁶ Consequently, the resulting monolayers on both surfaces are as closely packed as possible. The ball-and-stick model shows that the unit cells of the modified silicon surfaces have approximately the same size. Therefore, the electron density and thickness of the monolayer of **I** on the two surfaces will be similar as well.

Figure 6 shows the reflectivity data for the unprotected alcohol **V** (top) and the protected monolayer of **VIII** (bottom). The single layer best fits resulted in significant deviation from the data at large Q values and unreasonably high electron densities as seen in Table 2. From the IR-analysis of the alcohol-terminated monolayer (**V**)—vide supra—it was already clear that this alkene does not give

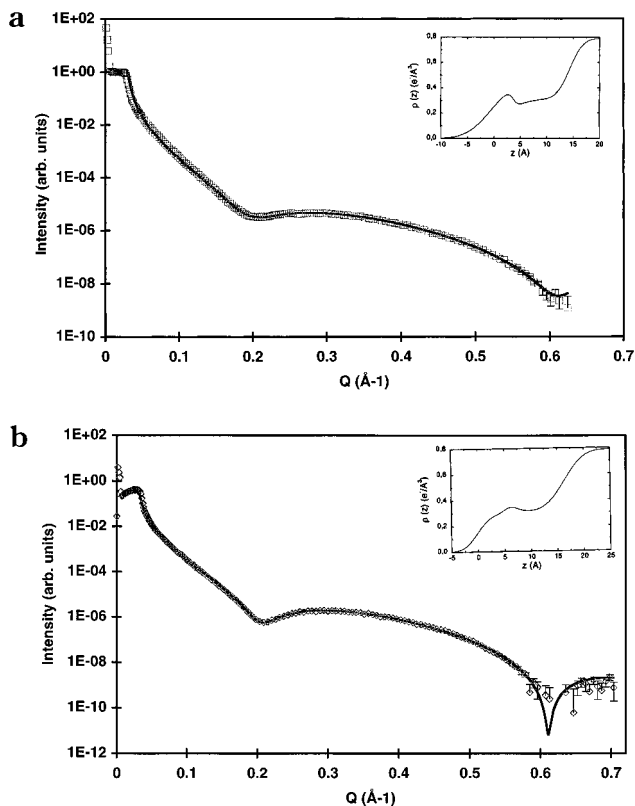


Figure 6. (a) X-ray reflectivity profile of a monolayer of **V** on Si(100). The inset shows the electron density profile as calculated from a three-layer model (see text). (b) X-ray reflectivity profile of a monolayer of **VIII** on Si(100). The inset shows the electron density profile as calculated from a three-layer model (see text).

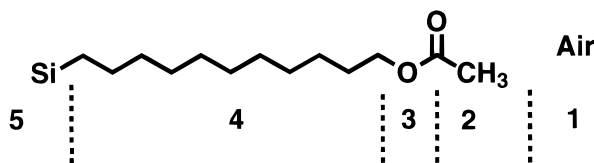


Figure 7. Schematic representation of the three-layer model for a monolayer on silicon, as used for the analysis of the X-ray data of a monolayer of **VIII** on Si(100). The numbers represent the number of each layer (air = layer 1) in the model. The same model was used for the monolayer of **V**, in which the end group is OH instead of an acetate group.

a closely packed monolayer. For the monolayer of **VIII**, a single layer model might be insufficient, because the acetate group in the monolayer is relatively electron-rich compared to the underlying alkyl chain. This can be accounted for by using a three-layer model, as schematically depicted in Figure 7.

The solid lines in Figure 6 are the best fits to a three-layer model, consisting of a chain of CH_2 groups on the substrate, a narrow electron-rich intermediate layer that corresponds to the oxygen atoms in the monolayer, and a cap layer (see Figure 7). The electron density of the first layer was fixed at $0.31 \text{ e}^-/\text{\AA}^3$, as determined previously from the alkyl monolayers of **I–III**. The insets show the resulting electron densities corresponding to the best fits. The resulting fitting parameters for each layer are listed in Table 3.

The total film thickness of 16.40 Å for the protected monolayer of **VIII** is consistent with the chain length. The peak electron density, 6.33 Å below the free surface, is smeared out to $0.35 \text{ e}^-/\text{\AA}^3$, because the interface roughness on both sides of this electron-rich intermediate

(45) Ewen, B.; Strobl, G. R.; Richter, D. *Faraday Discuss. Chem. Soc.* **1980**, *69*, 19.

(46) Asmussen, A.; Riegler, H. *J. Chem. Phys.* **1996**, *104*, 8151–8158.

Table 3. Monolayer Properties Derived for V and VIII from Best Fits Using a Three-Layer Model

parameter ^a	V	VIII
σ_{21} (Å)	3.8	2.0
t_2 (Å)	2.2	5.4
d_2 (e ⁻ /Å ³)	0.51	0.29
σ_{32} (Å)	2.1	1.2
t_3	1.5	1.1
d_3 (e ⁻ /Å ³)	0.46	0.43
σ_{43} (Å)	0.75	1.5
t_4 (Å)	10.7	9.9
d_4 (e ⁻ /Å ³)	0.31	0.31
σ_{54} (Å)	2.0	2.9

^a σ_{xy} = interface roughness of interface between layers x and y ; t_x is the thickness of layer x , d_x is the corresponding electron density.

layer is comparable to the thickness of the layer. The electron density of the cap layer is 0.29 e⁻/Å³, as expected for methyl termination.

For the monolayer of **V**, a total film thickness of 14.44 Å is still too high for a monolayer with this chain length. The peak electron density is 2.68 Å below the surface and has a value of 0.34 e⁻/Å³. Monolayer **V** is probably still contaminated, which yields an estimate of the film thickness that is too high. This result confirms the observation that the unprotected alcohol gives a disordered layer.

Functionalization of Ester-Terminated Surfaces.

The hydrolysis of ester-terminated monolayers would provide a convenient route to prepare alcohol- and acid-terminated surfaces, which cannot be prepared directly as shown above for compounds **IV** and **V**. Since these latter functional groups can be easily transformed into a variety of other functionalities, hydrolysis of the ester groups under relatively mild conditions would constitute an attractive route to highly functionalized monolayers. Because alkaline hydrolysis seriously damages the silicon itself, the surfaces were hydrolyzed in boiling acidified water for 20–30 min. The alkyl monolayers of **I–III** were perfectly stable under these conditions, as would be expected for hydrophobic surfaces, but were also not affected when a mixture of 9:1 (v/v) of 2-propanol/concentrated hydrochloric acid was used. Consequently, hydrolysis in acidic water should have no effect on the ester-terminated monolayers, apart from the desired hydrolysis of the ester groups. The infrared spectra (p-polarized) of the various stages of the hydrolysis of the methyl ester surface (**VI**) are depicted in Figure 8.

The first spectrum (Figure 8a) shows the original monolayer of **VI**. The carbonyl stretching vibration is clearly visible at 1743 cm⁻¹. Upon hydrolysis, the spectrum changes considerably (Figure 8b). The anti-symmetric methylene stretching vibration has shifted to 2926 cm⁻¹, and the carbonyl stretching region shows two peaks of about the same intensity, which can be assigned to the various vibrations of carboxylic acid groups. Because the surface was rinsed in water before wiping with chloroform, some carboxylate groups may be present as well. Unfortunately, a detailed analysis of the carbonyl region is complicated, because of the low signal-to-noise ratio (see also Experimental Section) and the appearance of peaks from residual water vapor. The signal at 1743 cm⁻¹ is still present but is decreased in intensity relative to the 1711 cm⁻¹ band (vide infra). This may indicate that not all the ester groups were hydrolyzed, which has been observed before.^{47,48} However, the peak could also

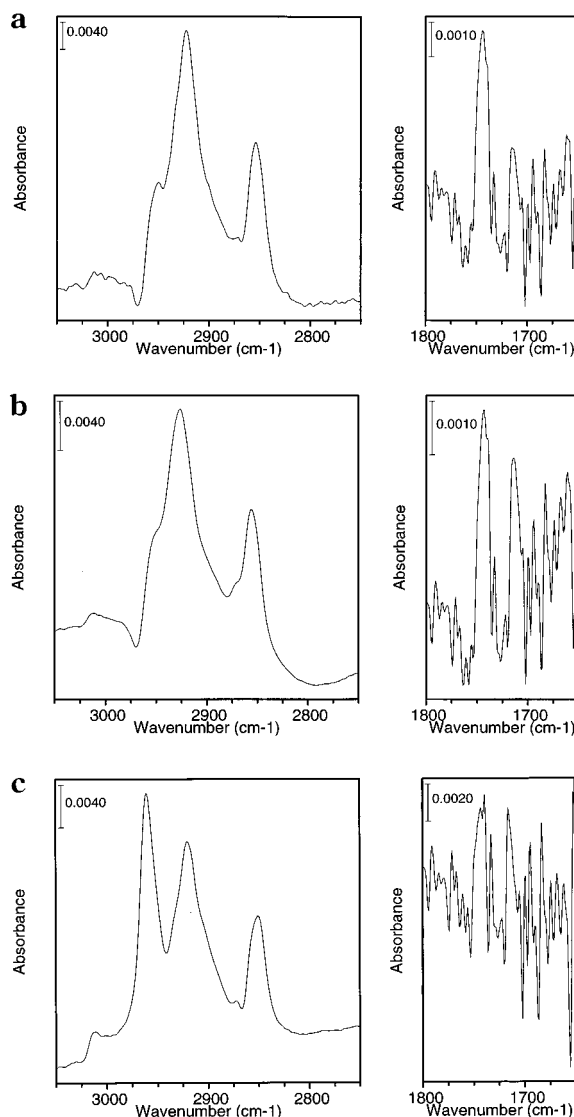


Figure 8. (a) Infrared spectra (C–H and C=O stretching regions) of a monolayer of **VI** on Si(100). (b) Infrared spectra (C–H and C=O stretching regions) of a hydrolyzed monolayer of **VI** on Si(100). (c) Infrared spectra (C–H and C=O stretching regions) of the monolayer of part b after subsequent reaction with acidic 1-propanol.

be assigned to non-hydrogen-bonded carboxylic acid groups,³⁵ which will be present if the acid-terminated surface reorganizes.³⁴ That hydrolysis did take place is evident from the water contact angles ($\Theta_{a/r} = 69/35^\circ$), which are lower than for the methyl-terminated surface and show a very large hysteresis. Directly after cleaning of the modified surface in water, small drops of water tend to spread on the surface, as would be expected for the hydrophilic, acid-terminated surface. Longer reaction times had no effect on the positions or intensities of the various peaks in the IR-spectrum.

The hydrolyzed monolayer was subsequently placed in acidified 1-propanol and heated to reflux for 30 min. The subsequently measured infrared spectra (maxima at 2920 and 2851 cm⁻¹; Figure 8c) and water contact angles ($\Theta_{a/r} = 83/75^\circ$) were very similar to the results of a monolayer prepared directly from the propyl ester (**VIII**). The carbonyl stretching region does not differ much from the hydrolyzed surface, still showing a peak at 1710 cm⁻¹. This small

(47) Fryxell, G. E.; Rieke, P. C.; Wood, L. L.; Engelhard, M. H.; Williford, R. E.; Graff, G. L.; Campbell, A. A.; Wiacek, R. J.; Lee, L.; Halverson, A. *Langmuir* **1996**, *12*, 5064–5075.

(48) Wasserman, S. R.; Tao, Y.-T.; Whitesides, G. M. *Langmuir* **1989**, *5*, 1074–1087.

peak at $\approx 1710\text{ cm}^{-1}$ was observed in all IR-spectra, also of the monolayers of **I–III**. The origin of this signal is, at present, unknown. Refunctionalization of the original ester surface is thus easily achieved. This observation also confirms that the ester groups do not react with the hydrogen-terminated surface and shows that the methyl ester **VI** gives an ordered monolayer.⁴⁹

Hydrolysis of the acetate surface (**VIII**) was expected to yield the hydroxy-terminated surface. Surprisingly, no changes were observed in either infrared spectra or contact angles after a reaction in boiling acidic water for 20 min. Replacing the water for ethanol lowered the contact angles by a few degrees to $\Theta_{a/r} = 71/62^\circ$ after 20 min, but longer reaction times had no further effect. Apparently the ester groups are not accessible and hydrolysis is not possible.

In contrast, reduction of the acetate surface (**VIII**) with LiAlH_4 (boiling ether, 15 min) does give the hydroxyl-terminated surface. A very hydrophilic surface is obtained directly after cleaning the modified surface with water, ethanol, and dichloromethane, with contact angles of about 20° , as estimated from small drops of water that were placed on the slightly tilted silicon sample. Measurement by the Wilhelmy plate method (see Experimental Section) showed a large hysteresis: $\Theta_{a/r} = 59/40^\circ$, confirming that the surface is more hydrophilic and that the acetate groups were removed. Infrared spectroscopy showed methylene stretching vibrations at 2923 and 2854 cm^{-1} and the complete disappearance of the $\text{C}=\text{O}$ vibration, in line with the complete reduction of the ester moiety.

Determination of Tilt Angles. More information about the precise structure of the monolayers can be obtained from the combination of the results from X-ray reflectivity and infrared dichroism. An average tilt angle, with respect to the surface normal, of the molecules in the monolayer can be calculated from the monolayer thickness as obtained from X-ray reflectivity, combined with the chain length of the molecule in the monolayer. The same tilt angle can be obtained from the results of infrared dichroism, if the infrared spectra are measured with s- and p-polarized light. The difference between the absolute absorptions of a certain vibration allows for the determination of this angle, using the formulas in the Experimental Section. Usually, the methylene stretching vibrations are used. Unfortunately, the error in the absolute absorbances can be as large as $\pm 10\%$, which makes this method often quite inaccurate.⁶ This error is also strongly affected by the variation in the absolute absorbances as a result of differences in the amount of absorbed contaminants on the background or the sample.⁵⁰ This can become an important factor for thin monolayers (e.g., monolayer of **III**), and for surfaces with polar groups, like **VI** and **VIII**, which get contaminated upon prolonged exposure to air. A second problem is the large dependency of α on the variation of D in the regions where $D \approx 1$ and

Table 4. Tilt Angles for Alkyl Monolayers of I–III on Silicon (100)^a

monolayer	$A_a^{s\text{-pol}}$ $A_a^{p\text{-pol}}$	α_a (deg)	$A_s^{s\text{-pol}}$ $A_s^{p\text{-pol}}$	α_s (deg)	Φ_{IR} (deg)	$\Phi_{\text{X-ray}}$ (deg)
I	0.071 0.068	72	0.047 0.042	90	18	29
II	0.074 0.075	64	0.042 0.043	63	39	26
III^b	0.0089 0.0096	58	0.0067 0.0058	90	32	26

^a $A_a^{s\text{-pol}, p\text{-pol}}$, absorbance of antisymmetric methylene stretching vibration using polarized light. $A_s^{s\text{-pol}, p\text{-pol}}$, absorbance of symmetric methylene stretching vibration using polarized light. α , angle between the surface normal and the symmetric or antisymmetric CH_2 dipole moment (see also Experimental Section). An α of 90° is assigned-to-dichroic ratios > 1.1 . Φ_{IR} , calculated tilt angle from IR-dichroism. $\Phi_{\text{X-ray}}$, calculated tilt angle from X-ray reflectivity.

^b Large uncertainty in the absorbances (see Table 1).

$D \approx 0$, corresponding to molecules that are oriented perpendicular and parallel to the surface, respectively.

Assuming that all the C–C bonds of the alkyl chain are in the trans-geometry, the film thicknesses of monolayers of **I–III** in Table 2 correspond to a constant tilt angle $\Phi_{\text{X-ray}}$ of $27 \pm 1.5^\circ$, calculated using the following expression:⁶

$$\Phi_{\text{X-ray}} = \cos^{-1}[(d - 0.77)/(2.52(n - 1)/2)]$$

where d is the measured film thickness and 2.52 \AA is the distance between next nearest carbons in an alkyl chain with n carbon atoms and 0.77 \AA is the covalent bond radius for C in a Si–C bond on the substrate.⁵¹ In the above formula for $\Phi_{\text{X-ray}}$ it is assumed that the Si–C bond is perpendicular to the silicon surface. From a ball-and-stick model of the silicon (100) surface, it is evident that this is not correct. However, variation of the Si–C bond angle with respect to the surface normal changes the resulting tilt angle of the alkyl chain by only $1\text{--}2^\circ$. This makes the above expression useful for the calculation of the approximate tilt angle, taking into account the uncertainty of $\pm 0.2\text{ \AA}$ in the monolayer thickness.

An estimated tilt angle for the alkyl chains of monolayers of **I–III** can also be obtained from the IR dichroism data. The resulting angles, Φ_{IR} , are listed in Table 4. For some monolayers, the dichroic ratio of the symmetric methylene stretching vibrations was found larger than 1.1, which gives unfeasible results in the calculation of α . A value for α of 90° was taken in these cases, because the value for α changes very rapidly for $D > 1$ and there is a large variation in D with changes of only a few percent in the measured absorbance. The tilt angles determined from the IR-dichroism vary between 18° and 39° . Though this is consistent with the results from X-ray reflectivity, such scattered values prevent drawing any conclusion from a combination of the two techniques.

X-ray reflectivity studies of arachidic acid on water indicate that the aliphatic tails are predominantly in the

(49) This monolayer has also been analyzed by X-ray reflectivity, using a commercially available 2 kW instrument (STOE&CIE GmbH, Darmstadt, Germany). A thickness of 13 \AA was found, in agreement with the chain length of this molecule and therefore indicative of a well-ordered monolayer. However, the X-ray reflectivity profile could not be measured accurately, because of a considerable contribution of the background to the signal intensity from approximately $Q = 0.35$, resulting in incorrect interface roughnesses ($\sigma_2 = 4$, $\sigma_3 = 0$) and an unreasonably high electron density of $0.42\text{ e}^-/\text{\AA}^3$.

(50) Care should be taken that the observed band heights are not altered as a result of contamination of the background crystal, a process that is quite fast. Small differences from background to background—and thus in the reported absolute absorbances of monolayers **I–III**—cannot be excluded, and the results from the dichroic ratio measurements should always be interpreted with caution.

(51) This value is slightly different from that previously used in ref 6, in which 1.86 \AA , corresponding to the Si–C bond length, was subtracted. Although a significant effect on the calculated tilt angle results (an increase of ca. 4°), the present approach is probably more reasonable, since the electron density will gradually change in the Si–C bond and not abruptly at the silicon surface. The film thickness as measured by X-ray reflectivity corresponds to the region between the air/monolayer interface and the monolayer/substrate interface. Since the latter interface is in the Si–C bond, the covalent radius of the Si atom is not included in the measured film thickness. See also refs 41a and 41b.

all-trans configuration and uniformly tilted.⁵² The tilt angle decreases continuously with decreasing area per molecule from 33° at 24 Å²/molecule to 0° at 20 Å²/molecule. Assuming that the tilt of the chains is completely determined by van der Waals interactions, a constant tilt angle of 27° suggests that the area/molecule is close to 24 Å²/molecule and that not all surface Si atoms are bonded to an alkyl chain. Another indication for this comes from the similar film thickness and electron density of **I** on the Si(100) and Si(111) surface. On the Si(111) surface only 50% of the silicon atoms is bonded to an alkyl chain.⁶ Although the Si(100) surface has a different structure and subsequently a different surface density of silicon atoms, it is still not possible to occupy all silicon atoms, as can be easily seen with a ball-and-stick model of the surface.

Reflectivity data for **VIII** also show a smooth film on Si(100). The film thickness of 16.40 Å, as calculated by the three-layer model, is comparable to the total chain length of the molecule. After subtraction of 0.77 Å for the covalent radius of the surface carbon atom, a tilt angle of 17° is found. The big ester functionality at the outside of the monolayer could force the alkyl chains to a more perpendicular orientation with respect to the surface.

Conclusions

The results presented above show that closely packed, well-ordered monolayers can be obtained by heating of a hydrogen-terminated silicon (100) surface to 200 °C in the presence of a 1-alkene. The monolayers prepared from long-chain alkenes (compounds **I–III**) are similar to those prepared on the silicon (111) surface,⁶ as evidenced by infrared spectra and X-ray reflectivity measurements. The advancing contact angles for water are similar as well, but the receding angles are somewhat lower, which is the result of surface roughness. It is well-known that, unlike the hydrogen-terminated silicon (111) surface, the silicon (100) surface is not atomically flat and consists of SiH, SiH₂, and SiH₃ groups.⁵³ Despite this surface roughness, dense monolayers can still be prepared. Stable monolayers can be formed over a wide range of alkyl chain lengths, as, e.g., the relatively short dodecene molecules (**III**) form an ordered monolayer. This shows that in this respect the monolayers are comparable to those of *n*-alkanethiols

on gold, which are ordered for $n > 9$,²⁶ and the monolayers on silicon oxide, which give ordered structures for alkyl chains that contain at least 12 methylene groups.⁵⁴

The possibility to use ω -functionalized alkenes opens the way to many interesting applications of this new method for monolayer preparation. However, dense monolayers cannot be obtained in all cases. Functional groups that can react with the hydrogen-terminated surface, like carboxylic acids (**IV**) and alcohols (**V**), give rise to disordered or even very poorly ordered monolayers. In contrast, well-ordered monolayers are obtained with the ester-protected analogues of these compounds (compounds **VI**, **VII**, and **VIII**). Enough space for the ester groups is available at the outside of the monolayer to allow for a dense packing. The observed contact angles show that the ester groups are indeed at the outside of the monolayer.

Because of the exceptional stability of the monolayers, when compared to the monolayers on gold and on silicon oxide, the protecting groups can be removed or modified, even when high temperatures are necessary. The conversion of the methyl ester-terminated surface of **VI** into that of the corresponding propyl ester (**VII**) proceeds smoothly and without any noticeable damage to the monolayer. The resulting surface was identical to that prepared directly from **VII**, which confirms that esters do not react with the hydrogen-terminated surface and that the functional groups are indeed at the outside of the monolayer. This provides a completely new pathway to the preparation of many functionalized surfaces that are currently not accessible.

The monolayers prepared from the allyl esters **IX** and **X** indicate that, unlike at the outside of the monolayer, not enough space is available for the ester groups near the silicon surface. Consequently, disordered monolayers are obtained.

Acknowledgment. This research was partially financed by The Netherlands Organization for Scientific Research (NWO) and The Netherlands Agency for Energy and the Environment (NOVEM). Mr. A. van Veldhuizen is gratefully acknowledged for help with the measurement of the NMR spectra. We also thank Mr. M. W. M. van Cleef and Dr. R. E. I. Schropp (Department of Physics, Utrecht University) for providing the silicon material.

LA971139Z

(52) Kjaer, K.; Als-Nielsen, J.; Helm, C. A.; Tippman-Krayer, P.; Möhwald, H. *J. Phys. Chem.* **1989**, *93*, 3200–3206.

(53) Dumas, P.; Chabal, Y. J.; Jakob, P. *Surf. Sci.* **1992**, *269/270*, 867–878.

(54) Hoffmann, H.; Mayer, U.; Krischanitz, A. *Langmuir* **1995**, *11*, 1304–1312.